NANO LETTERS

2007
Vol. 7, No. 3
729−732

Plasmon Resonances of a Gold Nanostar

Feng Hao, Colleen L. Nehl, Jason H. Hafner, and Peter Nordlander*

Laboratory for Nanophotonics, Department of Physics and Astronomy, M.S. 61, Rice University, Houston, Texas 77005-1892

Received December 17, 2006; Revised Manuscript Received January 18, 2007

ABSTRACT

Using the finite-difference time-domain method, we show that the plasmons of a nanostar result from hybridization of plasmons of the core and tips of the nanoparticle. The nanostar core serves as a nanoscale antenna, dramatically increasing the excitation cross section and the electromagnetic field enhancements of the tip plasmons. Our analysis demonstrates that the plasmon hybridization picture can be combined with numerical approaches to interpret the physical origin of the plasmons of highly complex nanostructures.

The plasmon resonances of a nanoparticle depend strongly on its composition and its shape.[1−4] The resonant excitation of plasmons can dramatically amplify the electric field near the nanoparticle surface. This phenomenon has key applications in surface-enhanced Raman scattering (SERS)[5,6] and also contributes to the strong sensitivity of the plasmon resonance to the local dielectric environment, which is exploited in localized surface plasmon resonance (LSPR) sensing.[7−11]

Of particular interest in SERS and LSPR sensing applications are tunable plasmonic nanoparticles, where the plasmon resonance can be placed at wavelengths where convenient laser sources are available.[12−17] Recently, a new type of nanoparticle, the nanostar, was synthesized and characterized using single-nanoparticle spectroscopy.[18] These particles are formed by seed-mediated, surfactant-directed synthesis, very similar to the synthesis method used for gold nanorods. The optical properties of the nanostars were found to be highly anisotropic and to strongly depend on the size of the protruding tips. The long wavelength plasmon resonances were also found to exhibit unusually large LSPR sensitivities, indicating the presence of large local electric field enhancements.

In this paper, we use the finite-difference time-domain (FDTD) method[19−21] to calculate the near- and far-field properties of a gold nanostar. The nanostar is modeled as a solid core with protruding prolate tips. The shape of this nanostar agrees qualitatively with the shape inferred from a scanning electron microscopy (SEM) image. The calculated extinction spectra agree very well with the experimentally observed scattering spectra for different polarization angles of incident light. While a computational method like FDTD is a powerful approach for calculating the optical properties of a nanostructure, it does not directly provide physical insight. Here we show that, by analyzing the spatial symmetry and wavelength dependence of the numerically calculated electric field enhancements, the physical nature of the nanostar plasmons can be elucidated.

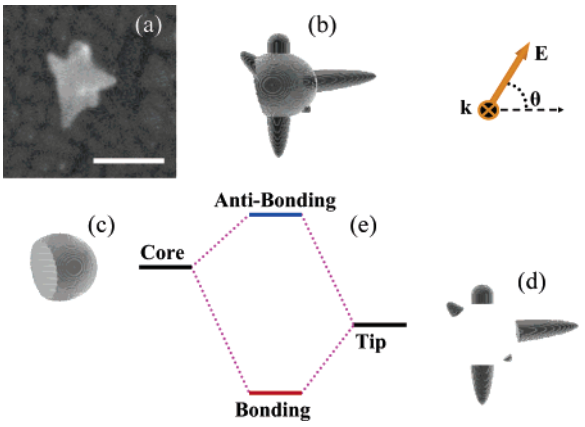

Figure 1. Structure of the gold nanostar investigated in this paper. Panel (a) shows an experimental scanning electron micrograph. The scale bar is 100 nm. Panel (b) shows the theoretical model, consisting of a truncated spherical core, (c) and tips, consisting of truncated prolate spheroids (d). Panel (e) illustrates the concept of plasmon hybridization in the nanostar. The core plasmons interact with the tip plasmons and form bonding and antibonding nanostar plasmons. The polarization angle is defined in the upper right corner.

The plasmon resonances of the nanostar result from the hybridization of plasmons associated with the core and the individual tips of the particle.[22,23] The low-energy bonding nanostar plasmons are primarily composed of tip plasmons but with a finite contribution of the core plasmons. The mixing in of the core plasmon mode dramatically increases the cross section for excitation of the bonding plasmons and results in very large local electric field enhancements compared to those that would be induced for individual tips.

* Corresponding author. E-mail: nordland@rice.edu. Fax: (713)348-4150.

10.1021/nl062969c CCC: $37.00
Published on Web 02/06/2007

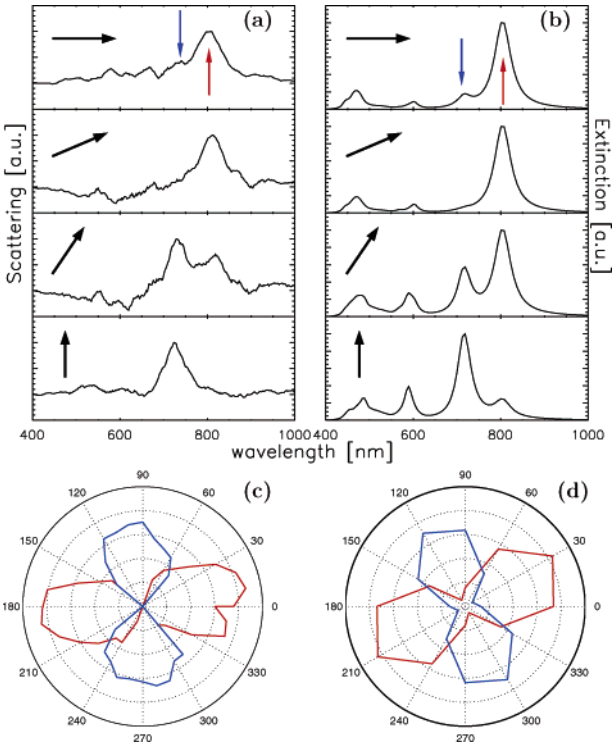

Figure 2. Experimental scattering (a) and theoretical extinction (b) spectra of the nanostar particle shown in Figure 1a−b for different polarizations of the incident light. The polarization angle θ varies from 0°, 30°, 60° to 90° and is indicated by the arrows in the panels. The bottom panels show the polarization dependence of the intensity of the two low-energy peaks indicated by the red and the blue arrows in panels (a) and (b).

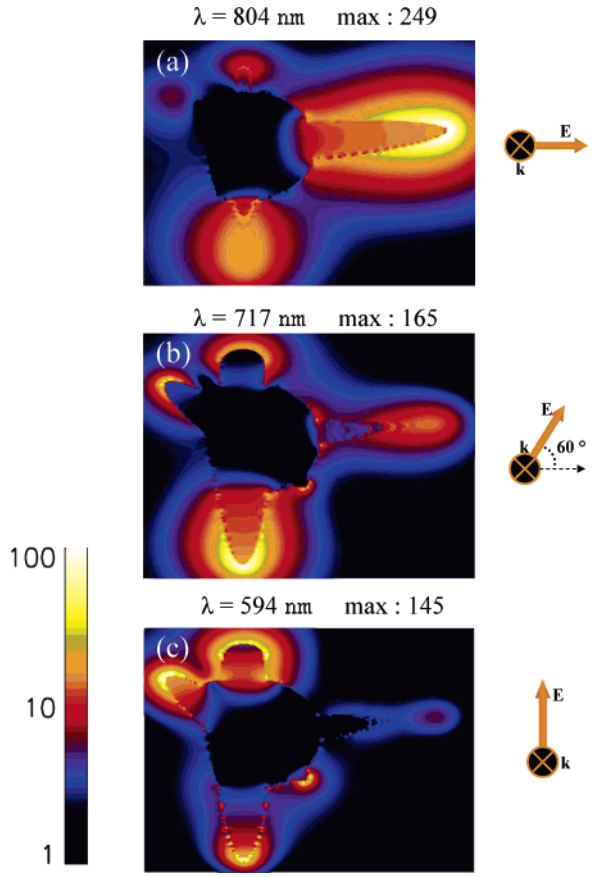

Figure 3. Color contour plots of the electric field enhancements for excitation of the (a) 804 nm, (b) 717 nm, and (c) 594 nm nanostar plasmon resonances. The polarization angles are indicated by the insets to the right of the panels. The maximum field enhancements are indicated on top of each panel.

In Figure 1, we show the SEM image of an experimentally synthesized nanostar particle and the simple theoretical model we propose. The nanostar is modeled as a truncated sphere with protruding tips of prolate spheroidal shape. For simplicity, all the tips are assumed to be pointing in directions within the same plane but have slightly different offset with respect to the center of the core in the direction perpendicular to the graph. This assumption does not alter the calculated spectra but simplifies the interpretation of the results and facilitates the graphical presentations of the electric field enhancements presented below. Specifically, the longest protruding tip on the right side of the nanostar can be tilted out of the plane of the paper without any significant change in the calculated spectra. All spectra are calculated for light incident perpendicular to the plane of the graph at a polarization angle θ defined in the inset of Figure 1.

In Figure 2, the experimentally measured scattering spectra are compared to the extinction spectra calculated using our FDTD method for different polarization angles of the incident light. Because of the large size of the gold nanostars, their extinction spectra are dominated by scattering, making a comparison between calculated extinction and experimental scattering possible.[24] The experimental spectra are characterized by two distinct peaks around 800 and 720 nm and weaker features at 650, 600, and around 500 nm. The theoretical spectra show two distinct resonances at 804 and 717 nm, a weaker feature at 600 nm, and several weak features around 500 nm. Our theoretical model for the nanostar was developed to account for the 800 and 720 nm resonances.

Both the experimental and theoretical spectra reveal that the effect of polarization angle is a change in the relative intensity of the peaks. This observation suggests that the different plasmon resonances of the nanostar are distinct plasmonic eigenstates of the particle and associated with the individual tips of the nanostar.

In the lower panels of Figure 2, the intensity of the 804 and 717 nm peaks are plotted as a function of polarization angle. The theoretically calculated angular dependence agrees well with the experimental data, indicating that our theoretical model for the nanostar is qualitatively correct. Because of the asymmetric orientation of the tips, several different nanostar plasmons can be observed for an arbitrary polarization of the incident light. The probability for excitation of a plasmon mode depends on the square of its dipole moment along the incident electric field.

In Figure 3, the calculated electric field enhancements for the three distinct nanostar plasmon resonances for polarization angles where the nature of the plasmon resonances become most apparent are shown. The planes of the plots are selected to bisect the centers of the respective tips. The electric field enhancement is defined as the electric field amplitude at a particular point normalized by the incident

electric field. Panel (a) shows the electric field enhancement for a polarization angle of $\theta = 0°$ and a wavelength of $\lambda =$ 804 nm. For this polarization, the extinction spectrum is dominated by the 804 nm plasmon resonance. This panel clearly reveals the existence of large surface charges on the horizontal tip. The calculated electric field enhancement is similar in magnitude to those found in junctions of nanoparticle dimers.[20] The field enhancements on the downward and upward pointing tips are very small, indicating that only very small surface charges are induced at this wavelength. The downward pointing tip appears smaller in size than in Figure 1 because it is centered in a plane located further inside the plane of the plot.

In Figure 3b, we show the electric field enhancements for a polarization angle of $\theta = 60°$. The contour plot for a wavelength of 717 nm illustrates that the surface charges associated with this particular plasmon mode are localized on the downward pointing tip. For this polarization angle, the extinction spectra show that both the 804 and 717 nm plasmon resonances can be excited. The field enhancements for a wavelength of 804 nm (not shown) look similar to those in Figure 3a with a maximum of 207.

In Figure 3c, we show the electric field enhancements for a polarization angle of $\theta = 90°$. The extinction spectra reveal two plasmon resonances, a strong peak at 717 nm, and a weaker feature at 594 nm. The field enhancements for the 717 nm mode (not shown) look similar to those in panel Figure 3b but with a larger maximum enhancement of 242. Panel (c) shows the field enhancement for the 594 nm mode. The plot shows that this mode is localized on the upward pointing tips with a substantial maximum field enhancement of 145.

The preceding discussion clearly shows that the different nanostar plasmons have significant surface charges associated with individual tips. We have also verified this explicitly by performing calculations on nanostars with single tips. The resulting spectrum only shows the plasmon resonances associated with that particular tip. The energies of a tip plasmon depend strongly on the aspect ratio of the tip and red-shift with increasing tip length.

We now analyze the plasmonic structure of the nanostar using the plasmon hybridization concept. The plasmon hybridization method is an analytical method that expresses the plasmons of a complex nanostructure in terms of the primitive plasmons of the elementary surfaces of the structure.[22,23] The complexity of the nanostar makes a straightforward application of the plasmon hybridization method impossible. Plasmons are incompressible deformations of the conduction electron distribution in the nanostructure. A characteristic feature of a plasmon mode is the appearance of oscillating surface charges that induce local electric fields. On an open-ended surface like that of a nanostar (in contrast to in a junction between two metallic surfaces), the induced electric fields are directly proportional to the surface charges induced by the collective plasmon oscillation. By analyzing the symmetry and the spatial distribution of the local electromagnetic field enhancements calculated using a numerical approach such as the FDTD method, the microscopic nature of the nanostar plasmons can be elucidated.

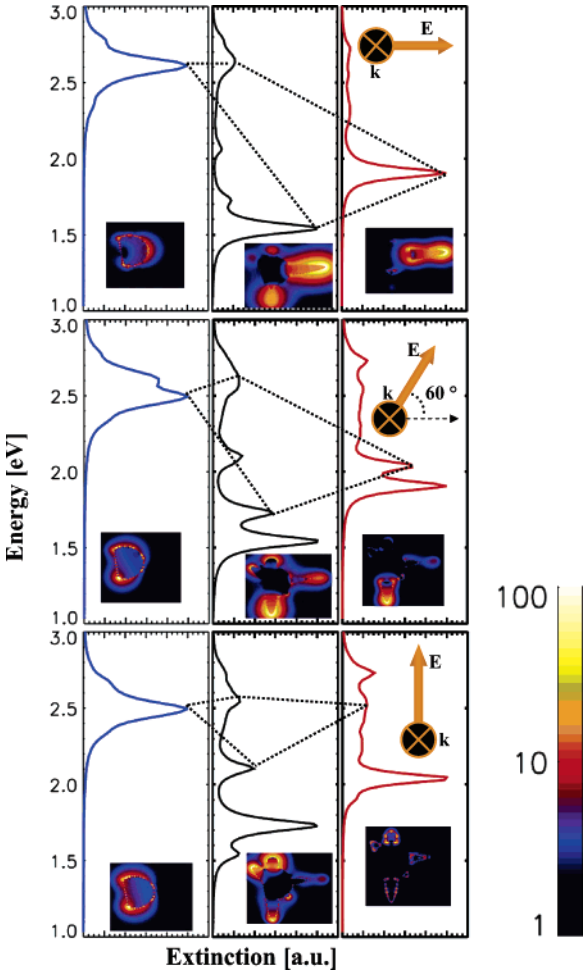

Figure 4. Microscopic origin of the three lowest nanostar plasmons. The left panels show the extinction spectra of the individual core. The right panels show the spectra of the tips. The middle panels show the extinction spectra of the interacting system. The dotted lines indicate the interactions that result in the bonding and antibonding nanostar plasmons. The contour plots show the electric field enhancements for resonant excitation of the different plasmon modes at the different angles. To make the extinction spectra more visible, the spectra for the core and tips have been multiplied by factors of 2 and 4, respectively. The same color scale bar is used in all the insets.

In Figure 4, we show the calculated extinction spectra for the individual core, the nanostar, and the individual tips for three different polarizations. The spectra are displayed as a function of energy. The color insets show the electric field enhancements of the structures for specific wavelengths. The extinction spectra for the core are shown in the left panels and are characterized by two plasmon resonances at 2.5 and 2.6 eV. The spectra show only a minor polarization dependence due to the relatively symmetric nature of the core. The electric field enhancements are distributed in a dipolar manner characteristic of the field enhancements for an almost spherical structure. The 2.5 eV plasmon resonance corresponds to a longitudinal plasmon resonance polarized parallel to the cut of the sphere, and the 2.6 eV mode is a transverse plasmon resonance polarized perpendicular to the cut.

In the right panels, we show the extinction spectra for the tips (without the core). It can be seen that these spectra depend sensitively on the polarization of the incident light. Because the tips are located at finite distances from each other, a weak interaction exists between the plasmons of the individual tips. The tip spectra thus consist of bonding and antibonding plasmon modes. In the following discussion, we will focus on the low-energy bonding tip modes that are localized on the individual tips. For an angle $\theta = 0°$, the spectrum displays a plasmon resonance around 1.9 eV. The field enhancement for this feature shows that it is a plasmon localized on the horizontal tip. The spectrum for a polarization angle $\theta = 60°$ exhibits two resonances, the same 1.9 eV resonance as was present for $\theta = 0°$ and a plasmon resonance at 2.1 eV. This plasmon resonance is associated with the bottom tip. The spectrum for $\theta = 90°$ shows the 2.1 eV resonance, associated with the bottom peak, and a weak feature at 2.5 eV, which is associated with the upper two tips.

The middle panels show the extinction spectra of the nanostar for different polarizations. Dotted black lines are used to denote how the core plasmon mode and tip plasmon mode hybridize to form bonding and antibonding nanostar plasmon modes. For a polarization angle of $\theta = 0°$, the transverse plasmon resonance of the core hybridizes strongly to form the bonding nanostar plasmon at 1.5 eV and an antibonding plasmon around 2.5 eV. The bonding mode is primarily composed of the low-energy tip plasmon. The red-shift of the bonding mode is larger than the blue-shift of the antibonding mode because the number of conduction electrons in the core is larger than in the tip. The panel for $\theta = 60°$ illustrates how the bonding 1.7 eV plasmon is formed by hybridization of the longitudinal core plasmon and the plasmon in the bottom tip. As discussed earlier, for this polarization, the bonding plasmon at 1.5 eV associated with the horizontal tip is also excited. The bottom panel shows how the 2.1 eV nanostar plasmon is formed by hybridization of the longitudinal core plasmon and the upper tip plasmons.

The hybridization of the core and tip plasmon increases the cross section for excitation of the bonding nanostar plasmons compared to the individual tip plasmons. The cross sections for excitation of individual tip plasmons are nominally a factor of 4 smaller than those for the bonding nanostar plasmons. The physical mechanism for this increase in cross section is the admixture of the core plasmons in the bonding nanostar plasmon modes. Because the core plasmons have larger frequencies than the tip plasmons, the conduction electrons of the core structure can adiabatically follow the lower-frequency tip plasmon oscillations. This coupling increases the effective dipole moment of the tip plasmons. The core structure thus serves as an antenna, both increasing the excitation cross sections and the electric field enhancements of the bonding nanostar plasmon modes. The electric field enhancements of the individual tip plasmons are around 185 (horizontal tip), 119 (lower tip), and 69 (upper tips) at their respective plasmon resonances. The corresponding enhancements for the bonding nanostar plasmons are 263, 242, and 145.

In conclusion, we have shown that the plasmon modes of a nanostar are formed by hybridization of plasmons associated with the core and the tips. We have demonstrated that the plasmon hybridization concept can be combined with a highly numerical electromagnetic approach to provide microscopic insight into the nature of the plasmon resonances of a complex nanostructure.

Acknowledgment. This material is based upon work supported by the U.S. Army Research Laboratory and the U.S. Army Research Office under contract/grant no. W911NF-04-1-0203, the Robert A. Welch Foundation under grants C-1222 and C-1556, and by NSF under grants EEC-0304097 and ECS-0421108.

References

(1) Averitt, R. D.; Sarkar, D.; Halas, N. J. *Phys. Rev. Lett.* **1997**, *78*, 4217−4220.
(2) Jensen, T. R.; Malinsky, M. D.; Haynes, C. L.; van Duyne, R. P. *J. Phys. Chem. B* **2000**, *104*, 10549−10556.
(3) Link, S.; El-Sayed, M. A. *J. Phys. Chem. B* **1999**, *103*, 8410−8426.
(4) Kelly, K. L.; Coronado, E.; Zhao, L. L.; Schatz, G. C. *J. Phys. Chem. B* **2003**, *107*, 668−677.
(5) Schatz, G. C.; van Duyne, R. P. Electromagnetic mechanism of surface-enhanced spectroscopy. In *Handbook of Vibrational Spectroscopy*; Chalmers, J. M., Griffiths, P. R., Eds.; John Wiley: Chichester, 2002; pp 1−16.
(6) Moskovits, M.; Tay, L.; Yang, J.; Haslett, T. *Top. Appl. Phys.* **2002**, *82*, 215−226.
(7) Sun, Y.; Xia, Y. *Anal. Chem.* **2002**, *74*, 5297−5305.
(8) Tam, F.; Moran, C.; Halas, N. J. *J. Phys. Chem. B* **2004**, *108*, 17290−17294.
(9) Raschke, G.; Brogl, S.; Sush, A. S.; Rogath, A. L.; Klar, T. A.; Feldman, J.; Fieres, B.; Petkov, N.; Bein, T.; Nichtl, A.; Kurzinger, K. *Nano Lett.* **2004**, *4*, 1853−1857.
(10) Rindzevicius, T.; Alaverdyan, Y.; Dahlin, A.; Hook, F.; Sutherland, D. S.; Kall, M. *Nano Lett.* **2005**, *5*, 2335−2339.
(11) Li, K.; Stockman, M. I.; Bergman, D. J. *Phys. Rev. Lett.* **2003**, *91*, 227402-1−227402-4.
(12) Oldenburg, S.; Averitt, R. D.; Westcott, S.; Halas, N. J. *Chem. Phys. Lett.* **1998**, *288*, 243−247.
(13) Aizpurua, J.; Hanarp, P.; Sutherland, D. S.; Kall, M.; Bryant, G. W.; de Abajo, F. J. G. *Phys. Rev. Lett.* **2003**, *90*, 57401.
(14) Murphy, C. J.; San, T. K.; Orendorff, C. J.; Gao, J. X.; Gou, L.; Hunyadi, S. E.; Li, T. *J. Phys. Chem. B* **2005**, *109*, 13857−13870.
(15) Wang, H.; Brandl, D.; Le, F.; Nordlander, P.; Halas, N. *Nano Lett.* **2006**, *6*, 827−832.
(16) Romero, I.; Aizpurua, J.; Bryant, G. W.; de Abajo, F. J. G. *Opt. Express* **2006**, *14*, 9988−9999.
(17) Shvets, G.; Urzhumov, Y. A. *Phys. Rev. Lett.* **2004**, *93*, 243902.
(18) Nehl, C. L.; Liao, H.; Hafner, J. H. *Nano Lett.* **2006**, *6*, 683−688.
(19) Oubre, C.; Nordlander, P. *J. Phys. Chem. B* **2004**, *108*, 17740−17747.
(20) Oubre, C.; Nordlander, P. *J. Phys. Chem. B* **2005**, *109*, 10042−10051.
(21) The FDTD calculations are performed with a Drude dielectric function with parameters fitted to experimental data for gold.[25] This fit accurately reproduces both the real and imaginary parts of the dielectric function of Au for wavelengths longer than 500 nm.
(22) Prodan, E.; Radloff, C.; Halas, N. J.; Nordlander, P. *Science* **2003**, *302*, 419−422.
(23) Wang, H.; Brandl, D. W.; Nordlander, P.; Halas, N. J. *Acc. Chem. Res.* **2007**, *40*, 53−62.
(24) A rigorous theoretical analysis of the scattering spectra of the nanostar would require a detailed modeling of the scattering geometry of the microscope and the effects of the substrate. Because the objective of the present paper is to provide a microscopic interpretation of the nature of the nanostar plasmon resonances, we focus on the computationally simpler extinction spectrum. The frequency and polarization dependence of the extinction and scattering spectra are known to be similar.
(25) Johnson, P. B.; Christy, R. W. *Phys. Rev. B* **1972**, *6*, 4370.

NL062969C